

UNCLASSIFIED

AD NUMBER
ADB232278
NEW LIMITATION CHANGE
TO Approved for public release, distribution unlimited
FROM Distribution authorized to U.S. Gov't. agencies only; Proprietary Information; Aug 97. Other requests shall be referred to US Army Medical Research and Materiel Command, 504 Scott St., Fort Detrick, MD 21702-5012.
AUTHORITY
USAMRMC ltr, 19 Jan 2001.

THIS PAGE IS UNCLASSIFIED

AD _____

AWARD NUMBER DAMD17-96-1-6256

TITLE: A High Sensitivity Imaging Scintimammography System
(ScintiMAM)

PRINCIPAL INVESTIGATOR: Tumay Tumer, Ph.D.

CONTRACTING ORGANIZATION: NOVA Research and Development
Riverside, California 92507

REPORT DATE: August 1997

TYPE OF REPORT: Annual

PREPARED FOR: Commander
U.S. Army Medical Research and Materiel Command
Fort Detrick, Maryland 21702-5012

DISTRIBUTION STATEMENT: Distribution authorized to U.S. Government agencies only (proprietary information, August 1997). Other requests for this document shall be referred to U.S. Army Medical Research and Materiel Command, 504 Scott Street, Fort Detrick, Maryland 21702-5012.

The views, opinions and/or findings contained in this report are those of the author(s) and should not be construed as an official Department of the Army position, policy or decision unless so designated by other documentation.

19971230 029

DTIC QUALITY INSPECTED 5

REPORT DOCUMENTATION PAGE

Form Approved
OMB No. 0704-0188

Public reporting burden for this collection of information is estimated to average 1 hour per response, including the time for reviewing instructions, searching existing data sources, gathering and maintaining the data needed, and completing and reviewing the collection of information. Send comments regarding this burden estimate or any other aspect of this collection of information, including suggestions for reducing this burden, to Washington Headquarters Services, Directorate for Information Operations and Reports, 1215 Jefferson Davis Highway, Suite 1204, Arlington, VA 22202-4302, and to the Office of Management and Budget, Paperwork Reduction Project (0704-0188), Washington, DC 20503.

1. AGENCY USE ONLY (Leave blank)		2. REPORT DATE August 1997	3. REPORT TYPE AND DATES COVERED Annual (1 Aug 96 - 31 Jul 97)
4. TITLE AND SUBTITLE A High Sensitivity Imaging Scintimammography System (ScintiMAM)			5. FUNDING NUMBERS DAMD17-96-1-6256
6. AUTHOR(S) Tumay Tumer, Ph.D.			
7. PERFORMING ORGANIZATION NAME(S) AND ADDRESS(ES) NOVA Research and Development Riverside, CA 92507			8. PERFORMING ORGANIZATION REPORT NUMBER
9. SPONSORING/MONITORING AGENCY NAME(S) AND ADDRESS(ES) Commander U.S. Army Medical Research and Materiel Command Fort Detrick, Frederick, Maryland 21702-5012			10. SPONSORING/MONITORING AGENCY REPORT NUMBER
11. SUPPLEMENTARY NOTES			
12a. DISTRIBUTION / AVAILABILITY STATEMENT Distribution authorized to U.S. Government agencies only (proprietary information, August 1997). Other requests for this document shall be referred to U.S. Army Medical Research and Materiel Command, 504 Scott Street, Fort Detrick, Maryland 21702-5012.			12b. DISTRIBUTION CODE
13. ABSTRACT (Maximum 200) The focus of this project is the early and accurate detection of breast cancer by reducing errors in breast diagnostic imaging. The technique uses the fact that malignant breast tumors uptake certain radionuclides that benign masses do not. The malignant tumor will be imaged by a ScintiMAM instrument that will have 3-dimensional imaging capabilities. It will also be collimatorless, which will increase its efficiency over the standard type of gamma-camera. It is a Compton camera, measuring the Compton scattering angle in the detector. It will also have high energy resolution, enabling it to ignore events that occurred from scatter within the breast. A key component of the system is a mixed-signal Application Specific Integrated Circuit (RENA chip) for read-out of the many detector channels. Much of the first year was spent on the development and testing of the RENA chip. The first version was found to have a noise levels of 150 e- rms testing it with a pulser and 400 e- rms in Am-241 spectra taken with a CdZnTe detector. A new version of the RENA chip was sent in for prototype fabrication. This new version will have more functionality and is expected to be even lower in noise.			
14. SUBJECT TERMS Mammography			15. NUMBER OF PAGES 23
			16. PRICE CODE
17. SECURITY CLASSIFICATION OF REPORT Unclassified	18. SECURITY CLASSIFICATION OF THIS PAGE Unclassified	19. SECURITY CLASSIFICATION OF ABSTRACT Unclassified	20. LIMITATION OF ABSTRACT Limited

FOREWORD

Opinions, interpretations, conclusions and recommendations are those of the author and are not necessarily endorsed by the U.S. Army.

____ Where copyrighted material is quoted, permission has been obtained to use such material.

____ Where material from documents designated for limited distribution is quoted, permission has been obtained to use the material.

____ Citations of commercial organizations and trade names in this report do not constitute an official Department of Army endorsement or approval of the products or services of these organizations.

____ In conducting research using animals, the investigator(s) adhered to the "Guide for the Care and Use of Laboratory Animals," prepared by the Committee on Care and Use of Laboratory Animals of the Institute of Laboratory Resources, National Research Council (NIH Publication No. 86-23, Revised 1985).

✓ ____ For the protection of human subjects, the investigator(s) adhered to policies of applicable Federal Law 45 CFR 46.

____ In conducting research utilizing recombinant DNA technology, the investigator(s) adhered to current guidelines promulgated by the National Institutes of Health.

____ In the conduct of research utilizing recombinant DNA, the investigator(s) adhered to the NIH Guidelines for Research Involving Recombinant DNA Molecules.

____ In the conduct of research involving hazardous organisms, the investigator(s) adhered to the CDC-NIH Guide for Biosafety in Microbiological and Biomedical Laboratories.

Legun Turner for

Turner O. Turner
PI - Signature

8/28/97
Date

IV Table of Contents

I Font Cover	1
II Standard Form (SF) 298, Report Documentation Page.....	2
III Foreword	3
IV Table of Contents.....	4
V Introduction.....	5
V.1 Background.....	6
V.2 Scope of Research.....	6
VI Body of Report.....	8
VI.1 Description of the RENA ASIC Chip.....	8
VI.1.1 Construction of the new low noise RENA test station	9
VI.1.2 Preliminary test results of the prototype RENA chip	10
VI.1.3 Functionality	12
VI.1.4 Linearity and noise.....	13
VI.1.5 New Printed Circuit Board for RENA Chip mounting.....	16
VI.1.6 New JFET Probe.....	17
VI.1.7 New CZT Detector Setup	17
VI.1.8 New Test Results	18
VI.2 New Version of the RENA Chip	20
VI.3 CdZnTe Calorimeter detectors.....	20
VII Conclusion.....	21
VIII References.....	22

V Introduction

Mammography is the most effective means of detecting nonpalpable breast cancer. However, its specificity is only 20-30%, with a sensitivity of 85% (Khalkhali et al., 1992; Baines et al., 1986). One out of 2 to 6 biopsies performed following diagnosis by mammography are malignancies (Baines 1986, Tabor 1984). In physical examination results, one out of 5 to 9 biopsies are found to be malignant. Normally several biopsies are performed per lesion. It is important to improve the specificity of mammography to reduce observational and interpretational errors, patient trauma and disfiguration from unnecessary biopsies. It is also important to reduce health care costs by decreasing the number of unnecessary biopsies. To detect 100,000 non palpable cancers 500,000 biopsies were performed at approximately \$5,000 per biopsy, a total cost of \$2.5B. A reduction of 50% will save about \$1.2B per year. Therefore, a new diagnostic imaging technique that can be used as an adjunctive imaging modality to positive mammograms could aid in diagnosis, reduce interpretational errors and provide cost reductions.

Palpable mass abnormalities of the breast are often difficult to evaluate mammographically, especially in patients with fibrocystic change and dense or dysplastic breasts, therefore potential for making interpretational errors is large. About 35% of older women over 50 and 70% of the woman under 50 have dense breasts (Tabor 1993). For example, it is found that invasive lobular carcinoma in dense breasts can attain a size of several centimeters and may still lack mammographic signs. About 50% of all preinvasive cancers do not show mammographically significant calcifications (Holland et al., 1983), decreasing the chance of detecting malignant tumors. There are also mammographically occult breast cancers that are not on a mammogram (Holland, et al., 1983). This is a situation where interpretational error in mammography is close to 100%. Once a patient is found to have a condition in which mammography is difficult, the patient should be imaged by another modality.

Patients who are in a high risk category for the development of breast cancer (i.e., patients with a family history of breast cancer, patients with prior histologic evidence of cellular atypia, patients with a prior history of breast cancer who have undergone lumpectomy and radiation therapy) may be difficult to evaluate and follow mammographically because of a dense fibroglandular pattern of physical changes caused by radiation (Waxman et al., 1993a). Currently, the only established method to resolve such a dilemma is random tissue biopsies in a suspicious area which is usually attended by high nonmalignant-to-malignant biopsy ratios. These cases may be evaluated by a technique that is not affected by dense fibroglandular patterns.

It has been demonstrated that treatment of palpable breast masses may be adversely affected when the clinician delays biopsy (Burns et al., 1978, 1979; and Mann et al., 1983). Mann et al. (1983) demonstrated that a false negative mammogram may cause a considerable delay in the decision to biopsy a patient subsequently shown to have carcinoma of the breast. Such cases need significant improvement in mammography and/or another modality to supplement mammography.

For a positive mammogram it may be less traumatic and more cost effective to quickly follow up with a scintimammography to determine, on that patient's visit, if the lesion is cancerous. If it is found to be malignant, the tumor could be localized and biopsied (e.g. fine needle) using the same system.

It is important to diagnose metastatic tumors in other parts of the breast, as well as metastases in the axillary lymph nodes, allowing accurate staging of disease non invasively. This functionality will require a three dimensional imaging system. In addition, the proposed scintimammography system can be used to determine if all of the primary lesion has been removed.

A new high sensitivity three-dimensional scintimammography system is proposed as a complementing modality to mammography to solve the problems stated above. The system at

present is based on the higher malignant tissue uptake of Tc-99m SestaMIBI and/or Tl-201 chloride compared to benign masses (except for some highly cellular adenomas) shown by clinical trials (Waxman et al., 1989, 1990, 1993a, b; Campeau et al., 1992; Khalkhali et al., 1992, 1993a, b). Therefore, these radiopharmaceuticals can be used to help diagnose and differentiate breast tumors from benign growths. The Tc-99m SestaMIBI is found to be superior to Tl-201 by Waxman et al. (1993b) and Khalkhali et al. (1993b) has studied 578 patients with excellent sensitivity. Possible mechanisms for uptake of Tl-201 chloride into tumor cells include the action of the ATPase sodium-potassium transport system in the cell membrane which creates an intracellular concentration of potassium greater than the concentration in the extracellular space (Britten and Blank, 1968). Thallium is thought to be influenced significantly by this system in tumors (Muranake, 1981; and Sessler et al., 1986). In addition, a co-transport system has been identified which also is felt to be important in uptake of thallium by tumor cells (Sessler et al., 1986). The mechanism of Tc-99m SestaMIBI accumulation in tumors is not clear but appears to be related to a 170kDa P-glycoprotein which is a plasma membrane transport protein (Piwnicka-Worms, 1993).

V. 1 Background

The first detection of Tl-201 uptake of breast tumor was a serendipitous discovery (Cox et al, 1976). Hisada et al. (1978) also saw the same effect. Recently several researchers have carried out patient studies and shown the importance of Tc-99m MIBI and/or Tl-201 scintigraphy (Waxman et al., 1989, 1990, 1993a, b; Campeau et al., 1992; and Khalkhali et al., 1992, 1993a, b). One of the prospective studies of Tc-99m SestaMIBI showed a 94% sensitivity and 70% specificity for detecting malignant breast lesions in patients with abnormal mammograms or physical examinations (Khalkhali 1993, 1994a, b). Moreover, the positive predictive value of this study was 60% and the negative predictive value was 96%. In this study, the lesion sizes were on average $1.9 \text{ cm} \pm 1.7 \text{ cm}$ in diameter. In another study, a comparison of Tl-201 and Tc-99m SestaMIBI was done on in 26 patients with primary malignancy (Waxman 1993, 1994) again showing the potential utility of scintimammography. This study showed a higher sensitivity for lesion detection using Tc-99m MIBI in the primary lesion (100% vs 92%), and axillary lymph nodes (100% vs 86%), however specificity of breast primary lesions was less with Tc-99m MIBI (85% vs 100%). Recently equally encouraging results have also been reported for Tc-99m Methylene Diphosphonate (MDP) with a sensitivity of 92% and a specificity of 95% (Piccolo et al. 1995).

V. 2 Scope of Research

The proposed scintimammography system is a new approach to gamma ray imaging. It uses the Compton double scatter technique to determine the direction of the incident photon directly. This eliminates the requirement for a collimator and significantly increases the detection efficiency. The objectives of the proposed research and development are to build a fully functional prototype high sensitivity scintimammography system (see **Figure 1**) which will be capable of the following applications for breast cancer diagnosis, detection and treatment:

1. Differentiation of malignant tumors from benign masses and reduction of false negative biopsies performed due to interpretational errors common in mammography.
2. Detection of nonpalpable cancerous lesions in women who cannot be screened effectively by mammography.
3. Three-dimensional imaging of the malignant tumor(s) so that the lesion(s) can be located, immediately biopsied or locating wire tags can be placed for the surgeon.
4. Imaging during surgery for localization and surgical confirmation of the excised tumor or detection of remaining malignant tissue.

The technical objectives are:

Proprietary

1. Improve gamma ray detection efficiency to 5% - 10% a factor of 50 to 100 times higher than the present high resolution gamma cameras and reduce patient dose or observation time, respectively.
2. Achieve spatial resolution for locating point size tumors to ≤ 3 mm.
3. Determine the energy of the incident gamma ray with high resolution to discriminate scattered gamma ray background and enhance the image.
4. Produce three-dimensional images of the breast for locating cancerous lesions.

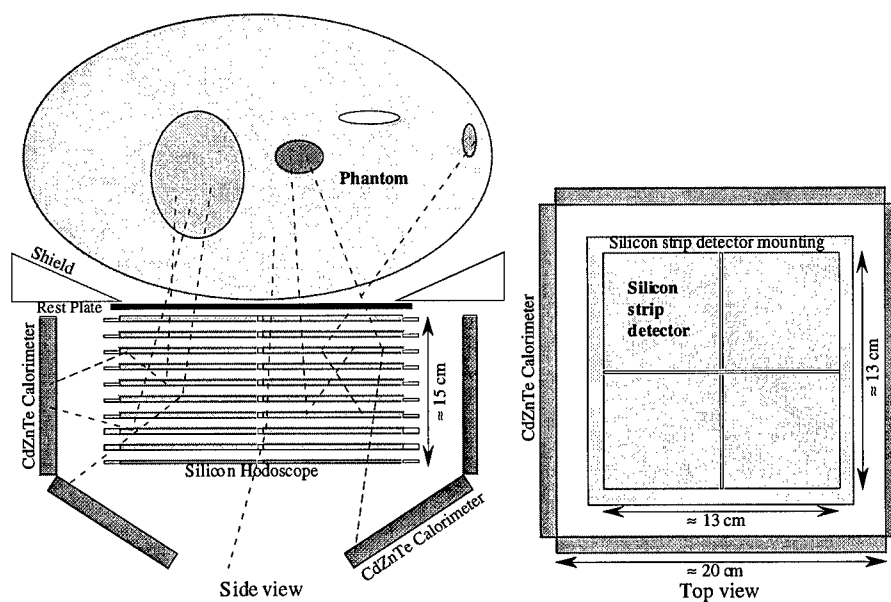


Figure 1. A preliminary diagram of the proposed prototype scintimammography system.

VI Body of Report

Due to the large number of detector channels that need to be read-out, one of the key components of the ScintiMAM system is the mixed-signal ASIC chip that will receive the charge signals from the Compton converter and calorimeter detectors. Using an ASIC as compared to discrete electronics makes ScintiMAM a viable device. Because of the ASICs' importance in this project, most of the first year was spent on the development and testing of the RENA (Read-out Electronics for Nuclear Applications) ASIC chip.

VI. 1 Description of the RENA ASIC Chip

The RENA chip is a multichannel signal processor with 32 detector inputs and associated signal processing channels. Each channel consists of an analog section and a digital section. There is an isolation analog channel at both edges of the analog channel group. Care has been taken to isolate the digital section from the analog section.

The following is a description of the analog signal processing path. The input stage is a re-settable charge integrator where a test charge can be injected. The signal from the input stage is switch controlled. The amplified signal is then shaped using a biquad Bessel filter which approximates a Gaussian response. The filter is implemented with a gm-C architecture consisting of transconductance amplifiers and capacitors. The shaped signal is amplified and peak detected. A sample and hold switch is used in the input to the peak detector circuit to isolate the peak detected signal from the input during the read out sequence. The threshold detector is an auto-zeroed comparator used to detect a valid trigger level. The trigger is input to the logic section. Another comparator is used to detect channel overload.

There are 32 control logic blocks, one for each detector channel. Each channel can be enabled or disabled, either for the calibration part or the whole channel. There is a 72 bit shift register which controls several of the chips modes of operation. Four address inputs are provided so that up to 16 RENA ASIC's may be daisy chained together using these inputs as static chip select lines. There are several ways for a channel control logic to be triggered as enumerated below.

1. A single channel is triggered by the associated analog signal channel through the IN(n). Simultaneous triggers may take place, but if any channel is triggered all other channel will be disabled by forcing ENTRIGB high. If EXT=0 there will be ~4 - 50 ns delay between a channel being triggered and other triggers being disabled. If EXT=1 the triggers will be disabled when TDIS pin goes high.
2. The Control Logic triggered by an external SELALL input to the IC which triggers all channels.
3. All channels are triggered by any channel being triggered. This mode of operation only takes place if Global Trigger Asserted.
4. If Near Neighbor Enable is asserted high, a neighboring cell will trigger the logic through IN_LPREV or IN_NEXT in this mode.

Data is read from the RENA chip in a sequential fashion. A triggered analog channel is selected on each read pulse edge and output to the SIGNAL pin. Each analog output has an associated address that is output at the same time as the analog signal to identify which channel is being read.

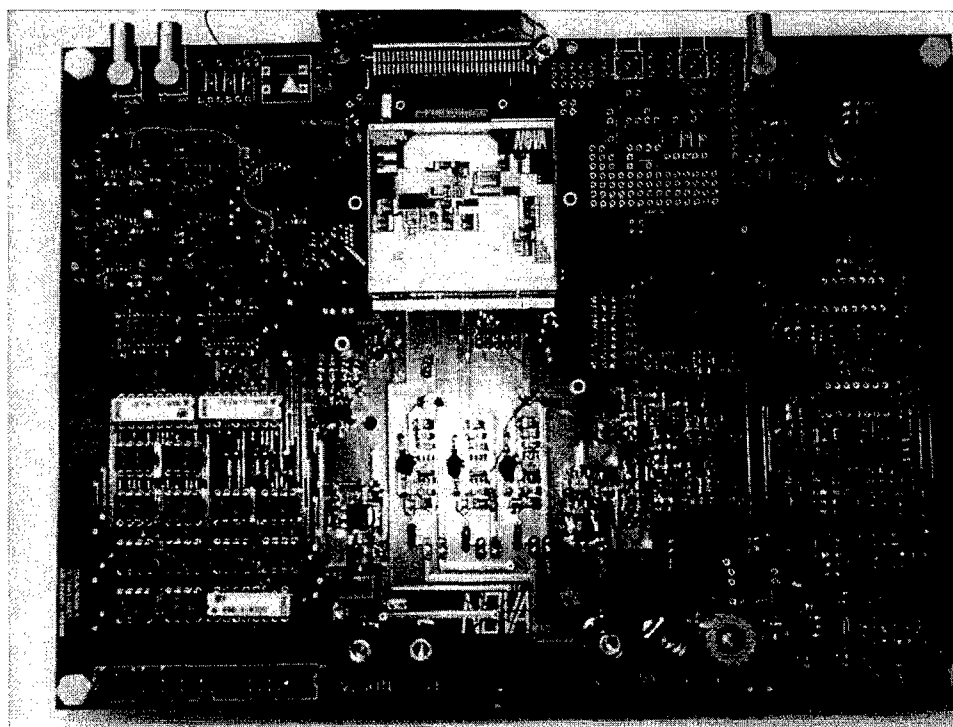
Proprietary

The final design was simulated and verified independently by NOVA's IC design consultants, and valuable corrections and improvements are adopted.

VI.1.1 Construction of the new low noise RENA test station

Photograph 1 is a photograph of the earlier version of the test system PCB board where digital and analog sections are all populated on one board. The analog signal section, the digital signal section and the reference voltage supply section were designed to be separated for isolation purposes. Each section has its own ground plane and the ground planes could be connected together through jumpers to find the best combination to achieve low noise. For the present test station, to achieve low noise, several such boards are used such that the analog and digital sections are populated on different boards and installed in different completely shielded metal boxes.

The new RENA chip requires a very low noise reference voltage supply, VRI, to achieve the low noise limits of the RENA chip. It is necessary for VRI to have a noise level of about 2 microvolts RMS. This reference voltage supply is vital to the noise measurements of the chip. A Hewlett Packard (HP) spectrum analyzer was used to measure the noise levels of the test station. It was found that the old test station had substantial noise problems. The noise levels were found to be from milli-volt to tens of microvolts at various frequencies. The highest noise source was determined to be from computer RF emission. **Figure 2** shows the block diagram of the new test station. Special consideration for low noise has been applied in both the schematic design and the Printed Circuit Board (PCB) layout.



Photograph 1. A photograph of the physical layout of the test station printed circuit board

Most of the noise sources has been identified and eliminated. For example, the communication and control lines between the data acquisition computer and the test station were entirely converted to fiber-optic cables. This technique has eliminated the computer RF emission problem and reduced the noise level on VRI from few milli volts RMS to tens of micro volts RMS. Application of the twisted pair cables between the digital control and analog control modules further reduced the noise level on VRI to about 20 micro volts.

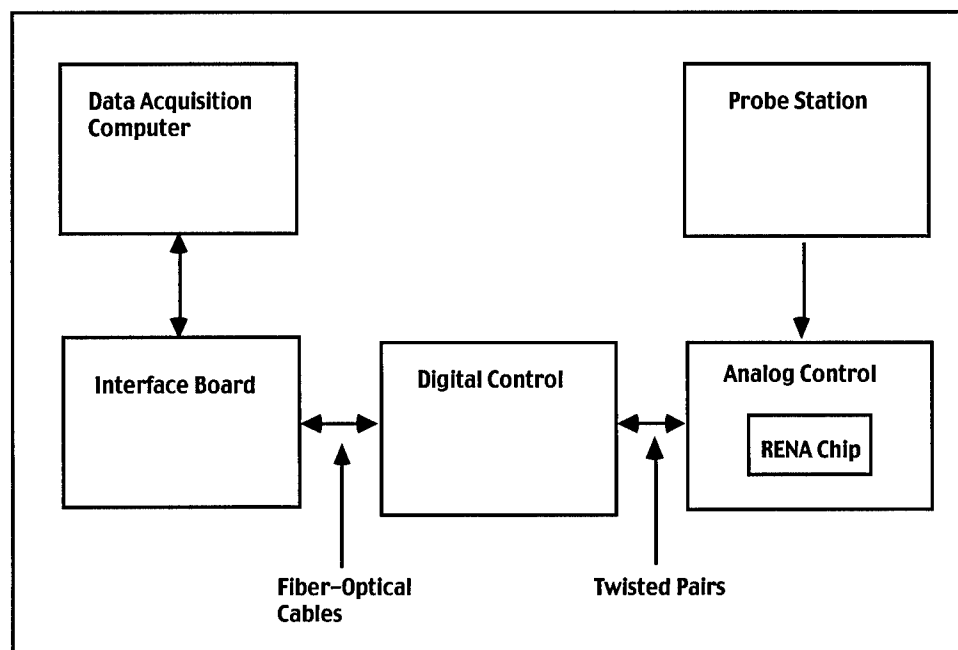


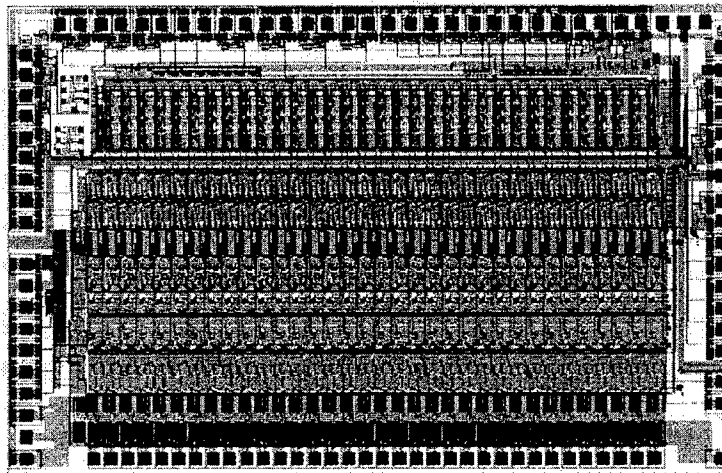
Figure 2 Schematic drawing of the RENA chip test station

VI.1.2 Preliminary test results of the prototype RENA chip

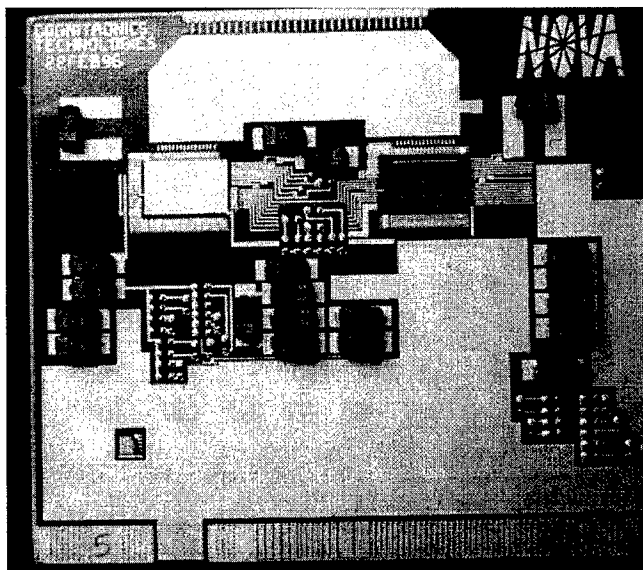
The new prototype RENA chips were fabricated using the HP 1.2 micron p-well CMOS process through the MOSIS service. **Photograph 2** is a photograph of the prototype RENA chip die where the actual chip size is 4.14 mm x 6.58 mm. Several test pads were placed on the chip so that the critical signal paths could be probed using a probe station.

The RENA chips are mounted individually on a ceramic carrier on which only passive components such as bypass capacitors and termination resistors are placed. Several ground planes are used for RF noise shielding. **Photograph 3** is a photograph of a RENA chip mounted on a dual chip ceramic carrier. The ceramic carrier is wire bonded onto the test station PC board.

Proprietary



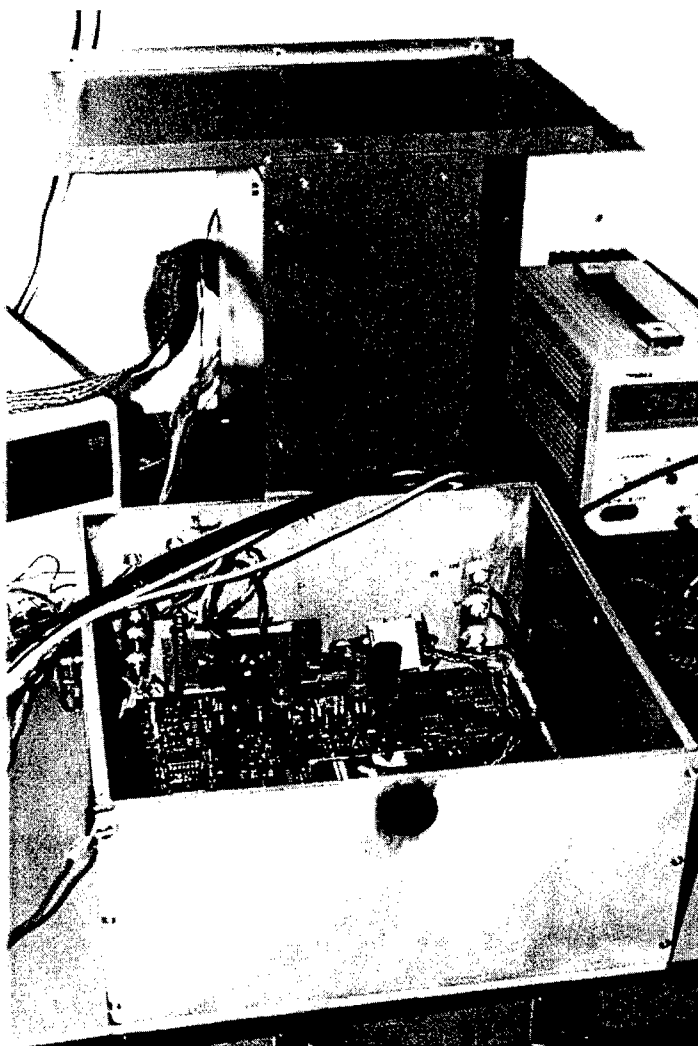
Photograph 2. A photograph of the prototype RENA chip showing the 32 actual plus 2 test channels.



Photograph 3. A photograph of a single RENA chip mounted on a dual chip ceramic carrier.

Proprietary

The test station PC board is enclosed in a 0.25 inch thick aluminum box for high quality RF interference shielding. All the feedthrough cables and power supply lines are carefully grounded and filtered to reduce the noise to a minimum level. **Photograph 4** is a photograph of the test station setup.



Photograph 4. A photograph of the prototype RENA chip test station setup.

VI.1.3 Functionality

All the operation modes, namely, Sparse Mode, Select All Mode, Global Trigger Mode, Nearest Neighbor Mode, and the External Delay are functioning. **Figure 3** shows a typical oscilloscope screen printout of several input and output pulses. In this figure four amplifier channels were enabled in which one channel has a real detector attached at its input, and it has a signal level higher than others. Oscilloscope trace #3 is the RENA chip analog output signal. Trace #2 is the Read Enable signal and trace #1 is the Read Clock signal where four read clock pulses are visible.

Proprietary

A minor design error, which prevents the Forced Enable feature of the chip from being functional, has been discovered. This error in the design does not effect the other read-out modes of the chip. It only prevents the Force Enable feature from turning on. The correction of this error has already been determined and two prototype RENA chips were been sent to a company where a special extremely accurate (at 1.2 micron level) cut-and-paste technique is used to correct this mistake. The cut-and-pasteoperation was succesfull and the force enable feature functions propoerly on these chips.

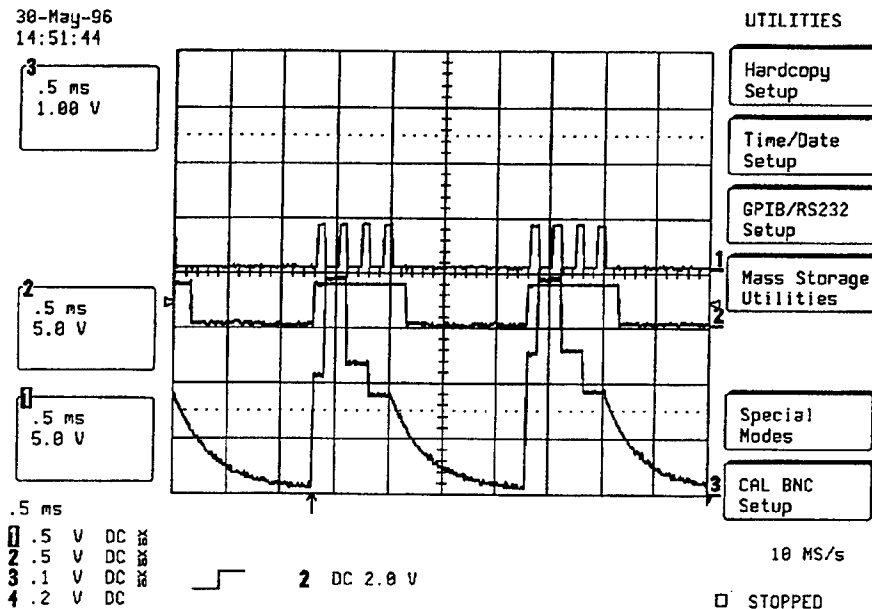


Figure 2. The typical input and output signals of a prototype RENA chip.

VI.1.4 Linearity and noise

The linearity and noise of the prototype RENA chips were measured. The noise at the output of the chip was measured by applying a pulse at the Calibration Input of the RENA chip. The system noise is determined by measuring the Full Width Half Maximum (FWHM) value of the output pulse. **Figure 4** is a plot from a Multi-Channel Analyzer (MCA), where the output pulse counts vs pulse height are plotted. Since the RENA chip has a designed output offset of about 1.6 volt, the lowest output pulse, which corresponds to zero input pulse or background, starts at about 1.6 volt or channel 210. The FWHM values of these pulses are about 3 channels, which corresponds to a system noise of about 300 electrons for this test station setup. This is already a major improvement by a factor of three over the NOVA's prevoius FEENA chip but about a factor of two higher than the design value. Therefore, further work is being carried out to reduce the overall system noise to the design specifications. The major contribution to this noise is believed to be from the test station PC board and not the RENA chip itself.

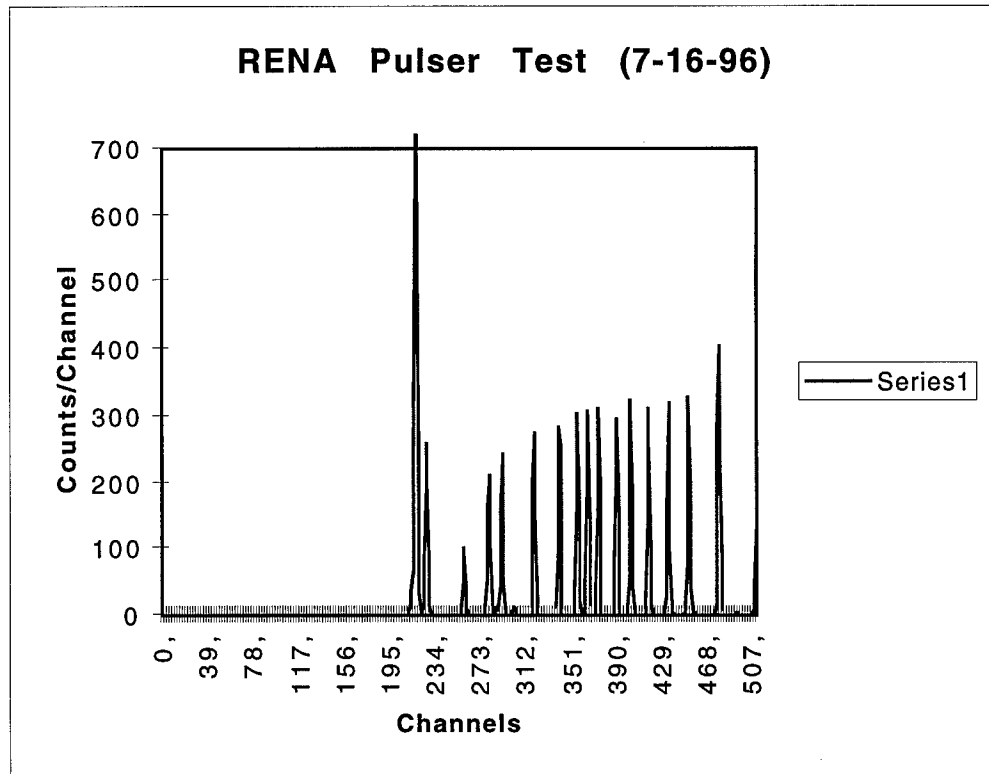


Figure 3. Noise measurements of the prototype RENA chip #4.

Figure 5 is a plot of a linearity measurement of RENA chip #4, where the chip analog output pulse height is plotted against the input pulse height. The slope of the curve is a measure of the chip gain and the deviation of the curve to a straight line is a measure of the chip linearity. A linear fit has been applied to the data points and the deviation of the data points to the straight line is measured to determine the linearity. We have obtained a linearity measurement of 4%, which is better than the best design value of (5%).

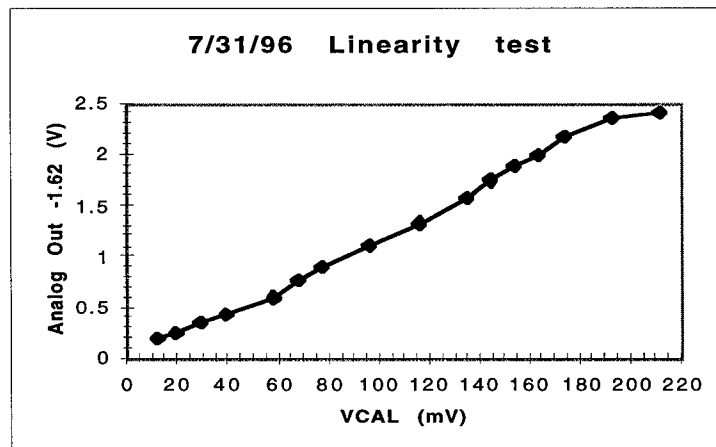


Figure 4. Linearity measurement of the prototype RENA chip #4

A CdZnTe detector was connected to the test station and irradiated with an ^{241}Am source. During the first trials, when the noise level was not reduced yet to the present levels, the energy spectrum obtained for the 59.8 keV ^{241}Am peak had a FWHM energy resolution of about 30 keV (**Figure 6**). The energy threshold was adjusted such that the counts below channel 20 were eliminated.

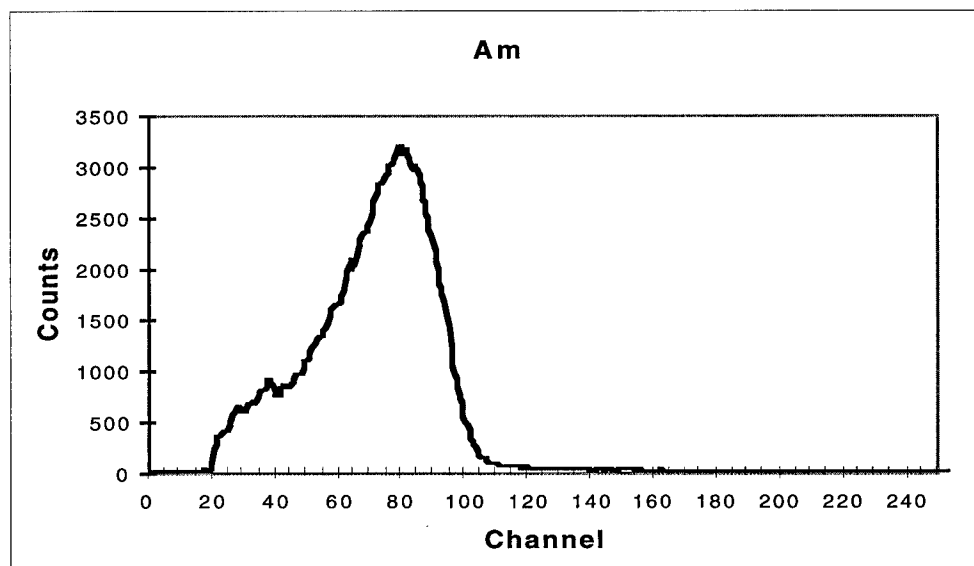


Figure 6. The ^{241}Am photopeak measured with a prototype RENA chip and the original test station without noise reduction.

Figure 7 shows the same spectrum with several noise reduction techniques applied as described above. The FWHM of the 59.8 keV photo peak is now about 9 keV, which is about a factor of 3 better than that of the spectrum in **Figure 6**, where no such noise reduction techniques were applied. Work on reducing the system noise further is still going on.

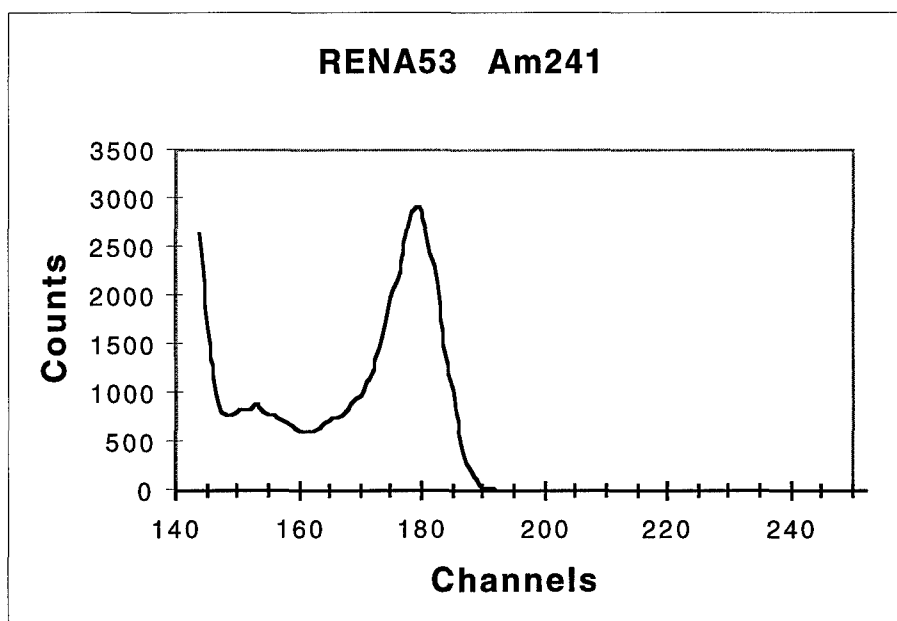
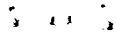


Figure 7. The ^{241}Am photo peak showing the noise improvement of the RENA test station.

To further improve the RENA chip test station a new test setup was constructed. Below is a description of this new test setup.

VI.1.5 New Printed Circuit Board for RENA Chip mounting.

A new printed circuit board was designed, fabricated and tested. This printed circuit board replaces the ceramic carrier previously used for mounting the RENA chip. It was especially designed for low inductance connections from the RENA chip to voltage references and the ability to place decoupling capacitors close to the RENA chip. The low inductance connection aid in keeping the voltage references the same (at the micro-volt level) on and off the RENA chip. It is a four layer board with the top and bottom layers containing routing traces and the inner layers containing ground and power planes. **Photograph 5** is a photograph of the above described board populated with a RENA chip and discrete components. This board is used in conjunction with the same analog board, described in the previous report, that had the ceramic carrier on it. It essentially replaces the ceramic carrier.



• • •

• • •

• • •

• • •

• • •

VI.1.8 New Test Results

One of the most revealing tests was measuring the RENA chip output noise level v.s. input capacitance load. This measurement can be performed in two ways: 1) by placing a capacitance between the input of the chip and the chip voltage reference VRI (located on the PCB board). Then varying this capacitance and measure the resulting output noise level. 2) By placing capacitors between the inputs of adjacent channels (which are referenced to VRI) and varying these capacitors and measuring the resulting output noise levels. The two test setups are shown schematically in **Figure 8**. The reasoning behind test setup 2 is that the relative difference of the reference voltage VRI between adjacent channels should be smaller than that between a channel and an external to the chip VRI. This difference may not seem significant, but when considering that VRI rms noise levels should be in the region of a few micro-volts, it is significant. Thus the second type of measurement gives a better evaluation of the intrinsic noise levels of the chip. **Figure 9** has the results from test setup 1 and test setup 2.

The results from test setup 1 has a much larger slope or corresponding noise figure of $56 \text{ e}^-/\text{pF}$ then does the results from test setup 2 ($8.3 \text{ e}^-/\text{pF}$). This is an indication that the noise level of the reference voltage VRI on the PCB board is too high and estimated to be 9 micro-volts from these measurements. Further improvements are necessary to lower the noise of VRI on the PCB board. The low absolute value of the slope from test setup 2 results indicate that the chip itself does not have noise problems and that the noise level of VRI on the chip is about 1.3 micro-volts

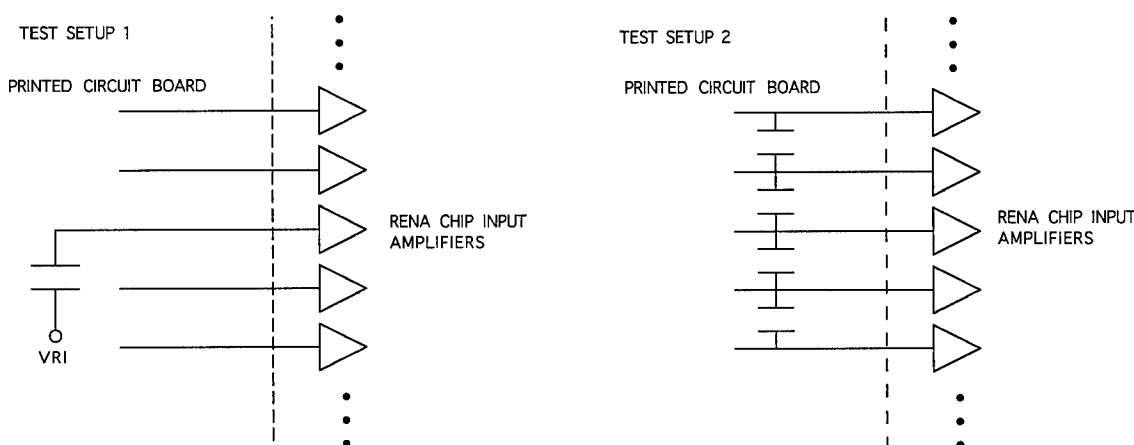


Figure 8. Schematic of the test setups 1 and 2 to measure RENA chip output noise v.s. the load capacitance.

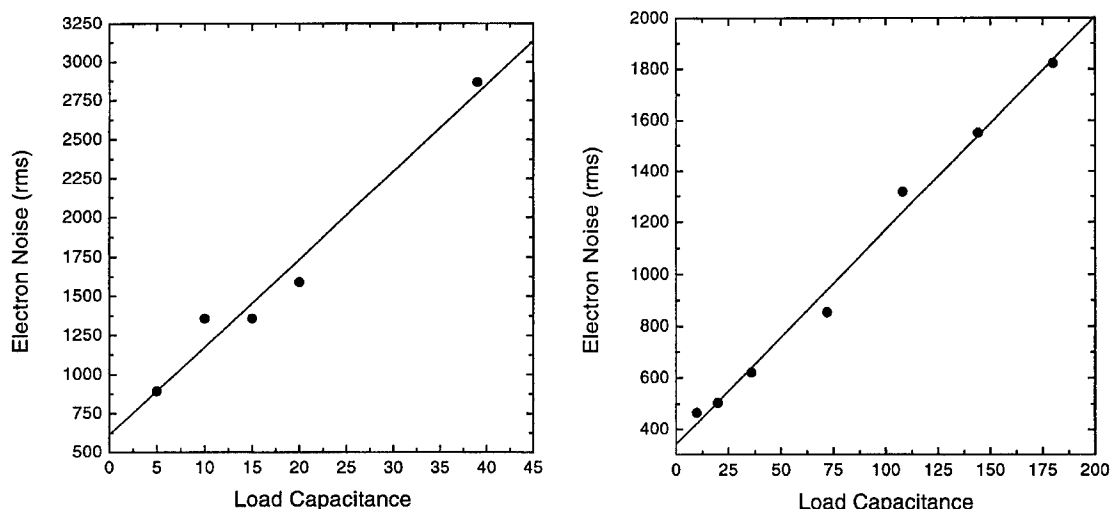


Figure 9. Measurements of RENA chip output noise v.s. input load capacitance. The figure on the left is for test setup 1 where the capacitor is referenced to VRI on the printed circuit board. The figure on the right is for the capacitors referenced to adjacent RENA input amplifiers (setup 2).

Further measurements on the gain linearity over the entire operating range of the RENA chip have been performed. The measurements were performed by supplying a pulse to the test input of the chip and measuring the voltage output. The results are shown in **Figure 10** and indicate that the linearity of the gain is very good. Also of importance is the slope of the linearity curve which yields the gain of the RENA chip. The chip designer estimated the gain for a test input pulse should be 12. The slope of the curve is 0.0124 (volts /millivolt) which gives a gain of 12.4, in good agreement with the predicted value.

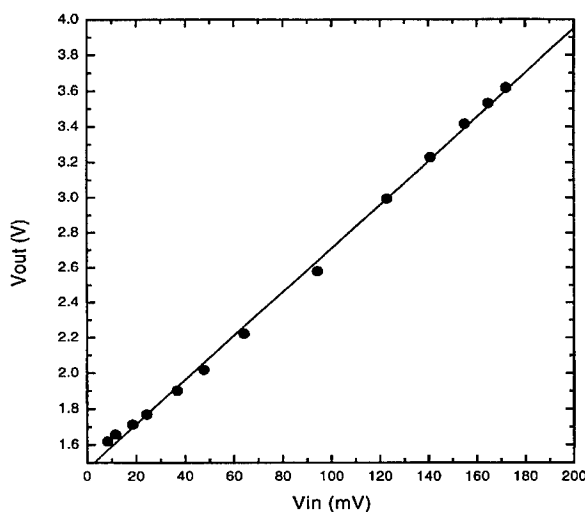


Figure 10. Output voltage v.s. input test pulse voltage gain curve.

With the new detector setup (described in section I.1.3) more spectra were acquired. One of these spectra are shown in **Figure 11** and shows a marked improvement over the spectrum in the previous report. The full-width-half-maximum of the new spectrum indicates a noise level of about 400 e⁻ RMS as calibrated with Am-241 and Co-57. This value is close to the practical limit of the noise associated with the detector as given by the detector manufacture's specifications.

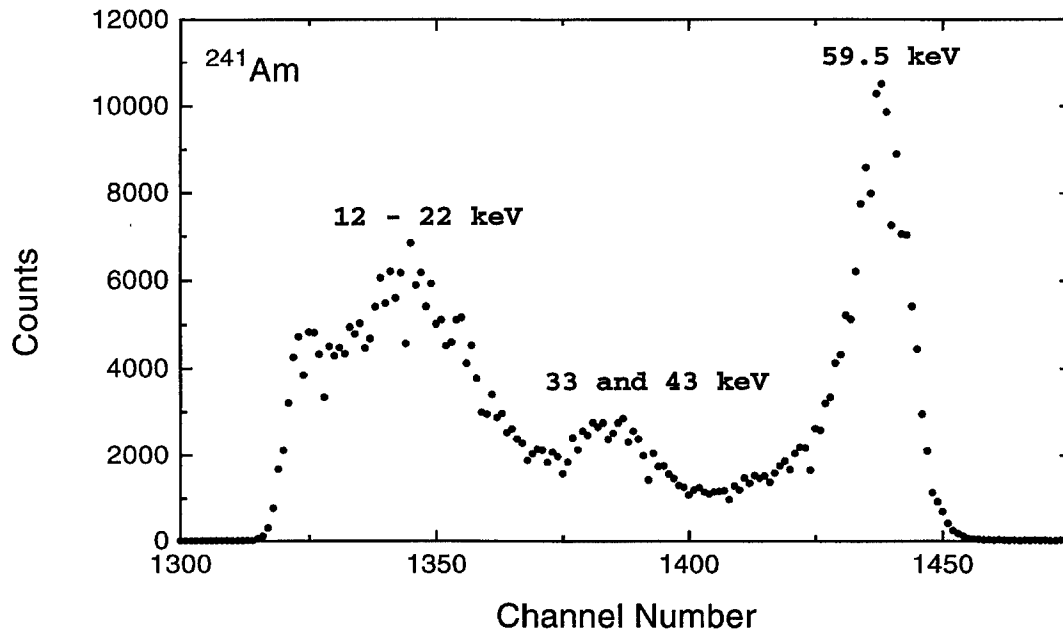


Figure 11. Energy spectrum of ²⁴¹Am obtained with the new detector setup.

Using the calibration input of the RENA chip and an pulser, the noise level was measured to be 150 e- RMS. These results are very encouraging and indicate that the RENA chip noise levels will be low enough to accomplish the resolution desired in the ScintiMAM instrument.

VI. 2 New Version of the RENA Chip

Even though the present version of the RENA chip is functional and has low noise levels, it was decided to make another prototype version before going into production with the RENA chip. This new version is presently under fabrication. The new version will: 1) correct the minor logic flaw that inhibited the force enable function, 2) decrease the dynamic range so that the RENA chip can better resolve lower energy gamma rays, 3) optimize the input amplifier for lower input capacitance and 4) include an additional read-out channel that can be used for pedestal subtraction and common mode noise reduction. We expect to receive the new prototype RENA chips in August of 1997 and begin testing as soon as possible.

VI. 3 CdZnTe Calorimeter detectors

The CdZnTe pad detectors that will be used for the calorimeter have started to arrive. A total of 8 have arrived and tested, of those 8, 4 had to be returned because most of the pads did not yield a signal. Of the 4 that were considered good only 1 or 2 pads out of 32 on each detector did not yield a signal. Am-241 spectra were acquired and the results were similar to the one shown in **Figure 11**. The CdZnTe pad detector test setup consists of a data acquisition and control computer, digital interface PCB board, detector PCB board, charge sensitive preamps and shaping amplifier. A spectra is acquired from each pad. The pad is selected by the computer and a bank of relays and the spectra is automatically saved. Testing the 32 channels takes about 15 minutes.

VII Conclusion

The RENA chip development has progressed very well, which is key to this project for its successful conclusion. It was shown to functionally work and low in noise. Because of the low noise requirements of the system several test setups had to be constructed before one could be used to test the low noise limits of the RENA chip. The new version of the RENA chip is expected to perform even better than the present version. This new version will arrive at *NOVA* in August and testing will begin in September and is expected to take about one month.

After testing of the new RENA chip is completed construction of the calorimeter consisting of RENA chips and CdZnTe pad detectors will begin. The ceramic carrier for the new RENA chip has already been designed, and has 0.5 mm pitch input pads, so that any detector with a pitch of 0.5mm or greater can be used with this carrier and aligned side by side. The Compton converter silicon strip detectors will use the same ceramic carrier for the RENA chip. Software development and for data acquisition from the new RENA chip and image processing has started.

VIII References

- Baines et al: Sensitivity and specificity of first screen mammography in the Canadian National Breast Screening Study: a preliminary report from five centres. *Radiology*, 160: 295-298, (1986).
- Britten, J.S. and M. Blank, "Thallium Activation of the (Na⁺, K⁺) Activated ATPase of Rabbit Kidney", *Biochim Biophys Acta* 15:160-166 (1968).
- Burns P.E., M.G. Grace, A.W. Lees, et al., "False Negative Mammograms Delay Diagnosis of Breast Cancer", *N Engl J Med*, 299:201-202, (1978)
- Burns P.E., M.G. Grace, A.W. Lees, et al., "False Negative Mammograms Causing Delay in Breast Cancer Diagnosis", *J Can Assoc Radiol*, 30:74-77, (1979).
- Campeau R.J., K.A. Kroemer, C.M. Sutherland, "Concordant of Tc-99m SestaMIBI and Tl-201 in Unsuspected breast Tumor", *Clin. Nucl. Med.* 1992 Dec; 17(12): 936-7.
- Cox, P.H., et al, *BJR*, 49:767 (1976).
- Hisada, et al. *Radiology* 129:497-500 (Nov. 1978).
- Holland R, Jan HC, Hendricks L, Mravunac M.: Mammographically Occult Breast Cancer: a Pathologic and Radiologic Study. *Cancer* 1983;52:1810-1819.
- Khalkhali, I., I. Mena, E. Jouanne, L. Diggles, B. Jackson, S. Klein, "Breast Cancer (Ca) Detection with Tc-99m-SestaMIBI Prone Imaging: Its Correlation with Mammography (MAMM) and Pathology", (Abstract), *Clinical Nuclear Medicine* Sep., Vol. 17, No. 9 (1992).
- Khalkhali, I., I. Mena, E. Jouanne, L. Diggles, K. Alle, S. Klein, "Tc-99m-SestaMIBI Prone Imaging in Patients (PTS) with Suspicion of Breast Cancer (Ca)", *Journal of Nuclear Medicine*, Vol. 24, No. 5 (May 1993a).
- Khalkhali, I., I. Mena, L. Diggles, Division of Nuclear Medicine, Harbor-UCLA Medical Center, Torrance, Ca., "Limitations of Mammography: The role of Tc-99m SestaMIBI Scintimammography in the diagnosis of Breast Cancer", (Abstract), *Clinical Nuclear Medicine* Oct., 1993, Vol. 18, No. 10 (also in 18th Annual Western Regional Meeting of the Society of Nuclear Medicine Oct 28-31, (1993b).
- Khalkhali I; Mena I; Jouanne E; Diggles L; Venegas R; Block J; Alle K; Klein S. Prone scintimammography in patients with suspicion of carcinoma of the breast. *Journal of the American College of Surgeons*, 1994a May, 178(5):491-7.
- Khalkhali et al: Clinical and Pathologic Followup of 100 Patients with Breast Lesions Studied with Scintimammography. *J Nucl Med* 35:P22, 1994b.
- Mann A.E., Giuliano, L.W. Bassett, et al., "Delayed Diagnosis of Breast Cancer as a result of Normal Mammograms", *Arch Surgery*, 118:23-25 (1983).
- Muranake, A., Accumulation of Radioisotopes with Tumor Affinity. II. Comparison of the tumor accumulation of Ga-67 citrate and Thallium-201 Chloride in vitro, *Acta Med Okayama*, 35:85-101, (1981).
- Piccolo, S., Lastoria, S., Mainolfi, C., Muto, P., Bazzicalupo, L., Salvatore, M., "Technetium-99m-Methylene Diphosphonate Scintimammography to Image Primary Breast Cancer, *J. Nucl. Med.* 1995: 36:718-724.

Proprietary

- Piwnica-Worms, D, Chiu M.L., Croop, J.M., Enhancement of Tc-99m-SestaMIBI accumulation in multidrug resistant (MDR) cells by cytotoxic drugs and MDR reversing agents, *Journal of Nuclear Medicine* 34: 140P, (1993).
- Sessler, M.J., P. Geck, F.D. Maul, et al., "New Aspects of Cellular Tl-201 Uptake: T+NA+-2Cl-Cotransport is the Central Mechanism of ion uptake," *Nucl Med* 25:24-27 (1986).
- Tabar, L. and Dean PB., Mammographic parenchymal patterns: risk indicator for breast cancer? *JAMA* 247: 185-189, (1982).
- Tabor, L., Okerland E, and God A., Five year experience with single view mamography randomised controlled screening in Sweden. *Rec Res Cancer Res* 90: 105-113, (1984).
- Waxman, Alan D., Lalthia Ramanna, Michael B. Brachman, et. al.: Thallium Scintigraphy in primary carcinoma of the breast: evaluation of primary axillary metastasis (abstract). *Clin Nucl Med* 14(Suppl):10,1989 also *J Nucl Med* 30: 844 (1989).
- Waxman, Alan D., Lalthia Ramanna, Leslie D. Memsic, et. al.: "Thallium Scintigraphy in differentiation of malignant from benign mass abnormalities of the breast", (abstract). *Clin Nucl Med* 15:769,1990 also *J Nucl Med* 31: 747 (1990).
- Waxman, Alan D., Lalthia Ramanna, Leslie D. Memsic, Clarence E. Foster, Allan W. Silberman, Stewart H. Gleischman, R. James Brenner, Michael B. Brachman, Christopher J. Kuhar, and Joseph Yadegar, "Thallium Scintigraphy in the Evaluation of Mass Abnormalities of the Breast", *The Journal of Nuclear Medicine* Vol.34 No. 1 (Jan, 1993a).
- Waxman, Alan D., G. Ashok, A. Kooba, J. Yadegar, M. Van Scoy-Mosher, L. Ramanna, A. Silberman and G. Rosen., "The Use of Tc-99m Methoxy Isobutyl Isonitrile (MIBI) in the evaluation of patients with Primary Carcinoma of the Breast: Comparison with Tl-201 (Tl)", (abstract). *The Journal of Nuclear Medicine Abstract book.*, No. 557, Vol. 34, page139p; (May 1993b).
- Waxman A, Nagaraj N, Ashok C, Khan S, Yadegar, J, Memsic L, Siberman A, Jochelson M, Katz R, Phillips D: Sensitivity and Specificity of Tc-99m Methoxyisobutal Isonitrile (MIBI) in the Evaluation of Primary Carcinoma of the Breast: Comparison of Palpable and Non-palpable Lesions with Mammography. *J Nucl Med* 35:P22, 1994.



DEPARTMENT OF THE ARMY

US ARMY MEDICAL RESEARCH AND MATERIEL COMMAND
504 SCOTT STREET
FORT DETRICK, MARYLAND 21702-5012

REPLY TO
ATTENTION OF:

MCMR-RMI-S (70-1y)

19 Jan 01

MEMORANDUM FOR Administrator, Defense Technical Information
Center, ATTN: DTIC-OCA, 8725 John J. Kingman
Road, Fort Belvoir, VA 22060-6218

SUBJECT: Request Change in Distribution Statement

1. The U.S. Army Medical Research and Materiel Command has reexamined the need for the limitation assigned to technical reports written for Grant DAMD17-96-1-6256. Request the limited distribution statement for Accession Document Numbers ADB232278, ADB257457 be changed to "Approved for public release; distribution unlimited." These reports should be released to the National Technical Information Service.

2. Point of contact for this request is Ms. Judy Pawlus at DSN 343-7322 or by email at judy.pawlus@det.amedd.army.mil.

FOR THE COMMANDER:

PHYLIS M. RINEHART
Deputy Chief of Staff for
Information Management